Acta Materialia 185 (2020) 518–527

Contents lists available at ScienceDirect

Acta Materialia

journal homepage: www.elsevier.com/locate/actamat

Full length article

The key role played by dislocation core radius and energy in hydrogen interaction with dislocations

Ping Yu[a], Yanguang Cui[b], Guo-zhen Zhu[c], Yao Shen[a,*], Mao Wen[a,*]

[a] School of Materials Science and Engineering, Shanghai Jiao Tong University, 800 Dongchuan Road, Shanghai 200240, China
[b] Shanghai Nuclear Engineering Research and Design Institute, 29 Hongcao Road, Shanghai 200233, China
[c] Department of Mechanical Engineering, University of Manitoba, 75A Chancellors Circle, Winnipeg, MB, R3T 5V6, Canada

ARTICLE INFO

Article history:
Received 15 May 2019
Revised 30 October 2019
Accepted 16 December 2019
Available online 19 December 2019

Keywords:
Hydrogen embrittlement
Hydrogen distribution
Dislocation
Monte Carlo technique
Atomistic simulation

ABSTRACT

It is generally believed that the H-induced reduction in dislocation energy plays a key role in modifying dislocation behaviors in the process of hydrogen embrittlement. Here, we examine the factors that lead to H reducing the line energies of the edge and screw dislocations in bcc Fe by atomistic simulations. Grand canonical Monte Carlo simulations are conducted to obtain the distribution of H around the dislocations. We find that H mainly aggregates at the dislocation cores and the H concentration in the elastic field of dislocations is extremely low. The direct consequences of such a distribution pattern of H are as follows. (i) In contrast with previous studies, H induces no change in the shear modulus of the systems containing dislocations. (ii) H increases the core radii and decreases the core energies of the dislocations, which are the only factors leading to the reduction of dislocation line energy by H. (iii) H brings little effect on the stress field of either the edge or screw dislocation, implying that H induces almost no stress-shielding effect on dislocations. A linear relation between the critical shear stress for homogeneous dislocation nucleation and logarithmic bulk H concentration is thus revealed, based on the atomistic result of the H-induced increase in the core radius and decrease in the core energy of the dislocations. The present results indicate that the dislocation-dislocation interaction in the presence of H, which is the key ingredient for the H-enhanced localized plasticity mechanism for hydrogen embrittlement, can be easily evaluated by the linear elastic theory of dislocations if the core radius and energy of dislocations are properly described.

1. Introduction

Hydrogen, as a promising solution for preventing the escalation of environmental problems from burning fossil fuels, has been attracting intense attention in recent years. A crucial issue for the practical application of hydrogen energy is the deleterious effect of H, called hydrogen embrittlement (HE) [1–3], that H degrades the mechanical properties of materials used for hydrogen storage and delivery system, such as high-pressure tanks and pipelines. Despite extensive studies over one hundred years, a complete understanding of HE has not been achieved yet.

Various mechanisms were proposed to explain the phenomenon of HE, based on extensive experimental studies and atomistic simulations, and it is now generally believed that the interaction of H with dislocations plays a crucial role in inducing HE [4–20]. Metallographic and fractographic observations provided evidences that dislocation emission from crack tips is enhanced by H [10–12]. In situ straining studies in an environmental transmission electron microscope (TEM) revealed that H speeds up the motion of dislocations, decreases the stacking fault energy, and stabilizes edge dislocations [13,14]. Recently, TEM observations using samples cut from crack tip by a focused ion beam instrument demonstrated that H-induced flat fracture surfaces are in fact associated with intensive local dislocation activities [15–17]. In situ electrochemical nanoindentation (ECNI) showed that H enhances homogeneous dislocation nucleation (HDN) [18–20].

The reasons for H affecting dislocation behaviors are closely related with H distribution around dislocations. Up to now, however, the distribution of solute atoms, including H, was usually evaluated based on their elastic interaction with the stress field of dislocations [21–25], or the binding energies of a single H atom with dislocations obtained from atomistic simulations [26–29]. Such schemes of evaluation ignored the atomic solute-solute (H–H) interaction, which is of key importance in determining solute (H) distribution in the dislocation core areas, where most

* Corresponding authors.
E-mail addresses: yaoshen@sjtu.edu.cn (Y. Shen), maowen@sjtu.edu.cn (M. Wen).

https://doi.org/10.1016/j.actamat.2019.12.033
1359-6454/

of solute (H) atoms are concentrated. In an effort to overcome this shortcoming, Pezold et al. [8] conducted atomistic simulations using an embedded-atom-method (EAM) potential reasonably describing the H–H interaction in the Ni lattice and found that the H–H interaction modifies the distribution of H around the edge dislocation. A direct consequence of the attractive H–H interaction in the Ni lattice is the formation of a local hydride in the core region of the edge dislocation. An effective "shielding" effect on the interaction between dislocations, which is the key ingredient of the well-recognized H-enhanced localized plasticity (HELP) mechanism for HE, can then appear at a bulk H concentration of only 160 appm. In the case of bcc Fe, however, there is still no detailed study on H distribution around dislocations.

The result of H binding with dislocations is a reduction in dislocation line energy [30–34]. Extensive experimental estimations of H binding energies with dislocations have been made for various materials [35–37]. Atomistic studies have provided more detailed information of a single H atom binding with dislocation cores [38–40]. The dislocation line energy E, in the frame work of linear elastic theory [41], is given by:

$$E = \frac{Kb^2}{4\pi} ln\frac{R}{r_c} + E_c, \quad (1)$$

where K is the energy factor determined by elastic constants, b is the magnitude of Burgers vector, and R and r_c are outer cut-off and core radius. The first term on the right-hand side is the dislocation line energy stored in the elastic region bounded by two circles of radii r_c and R, and the second term E_c is the dislocation core energy stored in the region bounded by the circle of radius r_c. Therefore, the H-reduced dislocation line energy can be attributed to H reducing K (or elastic constants) or E_c, or increasing r_c. Lu et al. [42], using the semi-discrete variational Peierls–Nabarro model with *ab initio* determined γ surfaces, provided the evidence that the core energies of all types of dislocations in Al are decreased by H. A recent atomistic study by Wang et al. [43] also showed that H decreases the core energies and modifies the core structures of both edge and screw dislocations in bcc Fe, when a line of equidistant H atoms were inserted into the binding sites near dislocation centers. Meanwhile, by loading the simulation boxes containing an edge or a screw dislocation, they observed that H only decreases the shear modulus of the box containing the edge dislocation. Barnoush et al. [18,19] studied the effect of H on HDN by ECNI experiments and found a significant decrease of the pop-in load by H. Based on the dislocation line tension model, they analyzed the influence of H on the line energy and concluded that the H-reduced pop-in load is mainly because of one of the results: H decreasing the shear modulus or increasing the core radius of dislocations, or the combined effect of them. However, the H solubility of the materials examined by Barnoush et al. [18,19] is very low, thus it is hard to believe that the shear modulus can be reduced by H. Therefore, the exact parameter that is modified by H remains to be uncovered.

In fact, even though a huge amount of experimental and atomistic studies have been conducted, there is still a lack of detailed atomistic studies on H distribution around dislocations in bcc Fe and the effect of H on dislocation properties. To this end, in the present study we first establish the distribution of H around $\frac{1}{2}[111](\bar{1}10)$ edge and screw dislocations in bcc Fe by performing grand canonical Monte Carlo (GCMC) simulations using our newly developed embedded-atom-method (EAM) potential for Fe–H system, which describes the H–H interaction in the bcc Fe lattice in according with DFT calculations up to the 12 shell binding site. The effects of H on stress field, energies and core structures of dislocations are evaluated and analyzed. The dependence of dislocation core radius and the critical stress for HDN on the bulk H concentration are then obtained following the elastic theory. Finally, the role of H-modified dislocation cores in dislocation activities is discussed.

2. Methods

2.1. Interatomic potential for Fe–H system

The accuracy of atomistic simulations relies on the interatomic potential adopted. To this end, we develop a Finnis–Sinclair EAM potential based on the Fe–Fe potential of Ackland et al. [44], which predicts the compact core structure of the screw dislocation in bcc Fe in accordance with density function theory (DFT) calculations. The Fe–H and H–H interaction parts of our potential are obtained by fitting globally to the database adopted from the DFT results of Ramasubramaniam et al. [45] and the H–H interactions in the Fe lattice from our DFT calculations, which is of crucial importance in describing H behaviors in the region of high H concentration. Details of the potential development can be found in the supplementary material. Our new EAM potential describes the H–H interaction completely in accordance with DFT results, while the H–H interaction of the previous EAM potential developed by Ramasubramaniam et al. [45] is always *attractive*. Such an attractive nature of the potential leads to unrealistic clustering of H atoms in simulations [46]. The main reason for this is that the H–H interaction of the potential beyond 0.9 Å was not optimized adequately.

As a further check, we calculate the elastic dipole of the individual H in bcc iron. According to the works of Clouet [47] et al., the elastic dipoles P can be calculated through $\sigma_{ij} = -\frac{1}{V}P_{ij}$, where V is the volume of the box and σ_{ij} is the stress tensor developed within the box containing a point defect. V and σ_{ij} can be directly evaluated from atomistic simulations. The obtained values are: P_{11}= 3.76 eV and P_{33}=3.36 eV. These are in close agreement with the DFT results of P_{11}= 4.33 eV and P_{33}=3.67 eV by Li et al. [48] using a 4 × 4 × 4 super-cell. Therefore, our potential describes the elastic field induced by H in the bcc Fe lattice reasonably.

2.2. Details of atomistic simulation

A cylindrical box is designed for simulations. The cylinder has a radius of 15 nm and a length of ~ 2 nm along the z direction. An edge dislocation is introduced into the box with the x, y, and z axes oriented along [111], $[\bar{1}10]$ and $[\bar{1}\bar{1}2]$, while a screw dislocation is introduced with x, y and z axes oriented along $[11\bar{2}]$, $[\bar{1}10]$ and [111]. The dislocations are arranged with line directions along the z axes and introduced by displacing all atoms according to the anisotropic elastic displacement fields calculated using the sextic formalism of Stroh [49]. Periodic boundary conditions are applied in the z directions. After the introduction of dislocations, the atoms in the outer shell of 13 Å thickness, i.e. two times of the cut-off distance of the Fe–Fe interatomic potential, are fixed while all other atoms are allowed to move freely during subsequent simulations. Relaxation by conjugate gradient (CG) method is then performed to obtain equilibrium dislocation structures.

We charge H into the whole simulation box except the fixed region at 300 K using the GCMC method [50] to obtain accurate H distribution around dislocations. In our GCMC simulations, the system is kept at constant chemical potential μ, volume V and temperature T. The bulk H concentration c_0 (in atomic fraction) is related with the μ of H by: $\mu = kTlnc_0 + \Delta E$, where ΔE is the energy change induced by inserting a H atom into the Fe lattice. The equilibrium distribution of H, thus, can be obtained by specifying the chemical potential μ and the temperature T.

There are three types of trial moves in GCMC simulations: the displacement of a randomly chosen atom, the insertion of a H atom at a randomly selected position and the deletion of a randomly chosen H atom. The displacement move is accepted or

rejected by the Metropolis algorithm and the insertion/deletion move is accepted or rejected by the algorithm of Adams [50]. However, application of the conventional GCMC technique to high-density systems, such as dense liquids or solids, is inefficient and difficult to reach convergence in reasonable time because of extremely low acceptance ratios of the insertion and deletion steps. It is for this reason that we apply the cavity-biased (CB) method of Mezei [51] in the present study, in which the insertion step is only attempted in the volume of cavities. The procedure of finding cavities is as follows: at a randomly selected site i, if all the separation distance between the site i and its neighboring atoms are larger than a prescribed value of r_{cut}, the site is considered to be inside of a cavity. Thus, the volume of cavities of the simulation system is just the probability of finding the cavities in the simulation box. At each insertion step in our simulations, 50 test attempts are made to check whether a randomly chosen site is inside a cavity using r_{cut} = 1.5 Å, and the probability of finding cavities is evaluated. By this technique, we get the successful acceptance ratio of ~1.5×10^{-3} for inserting a H into the box, which is about 4 times as many as the conventional MC method of ~3.8×10^{-4}. The fluctuation of H concentration during simulation is thus suppressed and the GCMC steps to reach equilibrium are decreased substantially. The attempted ratios for the displacement, insertion and deletion moves in our simulations are 50%, 25% and 25%, respectively.

Before charging H into the boxes containing dislocations, the dependence of c_0 on H chemical potential μ is determined by CB GCMC simulations at T = 300 K, using a periodic bcc box of $38a_0[100] \times 38a_0[100] \times 38a_0[100]$, where a_0 (2.8553 Å) is the lattice constant of Fe. Each simulation at an applied μ is run until the system reaches an equilibrium state. c_0 is then obtained by averaging over the microstates generated by the additional run of 10^5 GCMC steps per atom. A linear dependence of the natural logarithm of c_0 on μ, $lnc_0 = \mu/kT + 77.2804$, where k is the Boltzmann constant, is thus obtained.

Based on the obtained relation of c_0 with μ, H is then charged, with a prescribed μ (or c_0), into the box containing an edge or a screw dislocation by CB GCMC simulations. The charging process is restricted in region within R = 130 Å, which is 10 Å away from the fixed cylindrical boundary to eliminate the boundary effect on calculations, and is stopped when equilibrium is reached. Such a process usually requires 5×10^4 GCMC steps per atom.

In order to accurately evaluate the distribution of H and stress field around dislocations, and the dislocation line energies as a function of R from atomistic simulations, we locate the center of dislocations based on the Fe atoms near dislocation center. These atoms are identified by the deformation index (DI) method [52]. The DI of an atom i is defined as the maximum displacement relative to its nearest atom j: $DI_i = \max|\vec{r_{ij}} - \vec{r^0_{ij}}|/a_0$, where $\vec{r_{ij}}$ is the relative position vector of atom i and j and $\vec{r^0_{ij}}$ is the vector in the reference state. We define these heavily deformed atoms by the criterion of $DI \geqslant 0.3$. In the case of the edge dislocation, the x-coordinate of the dislocation center is obtained by averaging over all x-coordinates of the identified atoms, while the y-coordinate is the mean value of the separately averaged y-coordinates of the atoms above and below the slip plane. In the case of the screw dislocation, the dislocation center is defined as the circumcenter of the triangle comprised of three columns of high DI atoms.

3. Results

3.1. H distribution around dislocations

We subdivide dislocation boxes into $1 \times 1 \times L$ Å^3 small bins to obtain H distributions around dislocations as accurately as possible, where L the box length along the z direction. The H concentration c within a bin is calculated by $c = n_H/n_{Fe}$, where n_H is the number of H atoms and n_{Fe} the number of Fe atoms in the given bin. n_H is computed in each microstate generated by every 100 GCMC trial moves and averaged over 2.4×10^8 microstates. n_{Fe} is supposed to be homogeneous everywhere in the boxes and is thus evaluated by L/v_0, where v_0 is the atomic volume of Fe in perfect bcc lattice.

In order to obtain a continuous two-dimensional (2D) field of H concentration on the x–y plane, the H concentration in a bin i is smoothed using a coarse-graining procedure of [53]

$$\bar{c}_i = \frac{\sum_{\rho_j \leq \rho_c} c_j exp\left(-\frac{\rho_j^2}{\omega^2}\right)}{\sum_{\rho_j \leq \rho_c} exp\left(-\frac{\rho_j^2}{\omega^2}\right)}, \tag{2}$$

where c_j is the H concentration in the bin of j, ω the characteristic Gaussian width, and ρ_j the 2D separation distance between i and j within a critical distance of ρ_c. We use ω = 0.85 Å and the corresponding ρ_c = 1.5 Å, thus the smoothing procedure involves the bin i and its 8 neighboring bins. In the case of the edge dislocation, H distributions below and above the slip plane are calculated separately.

A typical core structure of the edge dislocation, obtained by averaging over 100 equilibrated snapshots, and the H distribution around the dislocation at c_0 = 1 appm are shown in Fig. 1(a). It is obvious that H accumulates at the tension region below the slip plane of the edge dislocation. The maximum H concentration is found at the sites on the $(\bar{1}10)$ atomic plane just below the slip plane, in agreement with the simulation result of the trapping site with maximum binding energy of H at the edge dislocation [29]. Since the core structure of the edge dislocation extends along the slip plane, as shown in Fig. 1(a), many deep trapping sites for H exist. Thus, H distributes along the slip plane widely. In order to quantitatively analyze the effect of H on the core structure of edge dislocation, the disregistry profiles (filled symbols) as well as the distribution of Burger vector (open symbols) are plotted in Fig. 2. It is clear that the H-charged disregistry curves and the distribution of Burger vector generally overlap with the H-free ones, indicating that H does not modify the core structure of the edge dislocation at low c_0.

The core structure of the screw dislocation without H, which is not shown here, is compact or non-degenerate, in accordance with the prediction by DFT [40]. At c_0 = 1 appm, as shown in Fig. 3(a), there is a minor change in the core structure. The core tends to extend along three {110} planes, resulting in the three-fold regions of high H concentration. The locations of maximum H concentration, as shown in Fig. 3(b), are at the sites with the maximum H binding energy, which is about 3 Å away from the dislocation center.

As a comparison, we also calculate the H concentration at a site near the dislocations according to Fermi-Dirac statistic

$$\frac{c}{1-c} = \frac{c_0}{1-c_0} exp\left(-\frac{E^{bind}}{kT}\right), \tag{3}$$

where E^{bind} is the bind energy between H and dislocation. E^{bind} can be obtained using either atomistic simulations or elasticity.

We first compute E^{bind} using atomistic simulations. The binding energy of H with dislocation is determined using molecular statics by:

$$E^{bind} = E_d + E_0^H - E_d^H - E_0, \tag{4}$$

where E_d is the total energy of the system containing a dislocation, E_0^H is the total energy of perfect bulk with one interstitial H atom at tetrahedral site, E_0 is the energy of the reference perfect bulk, and E_d^H is the total energy containing one dislocation and one H atom. We then calculate H concentration at each site using Eq. (3),

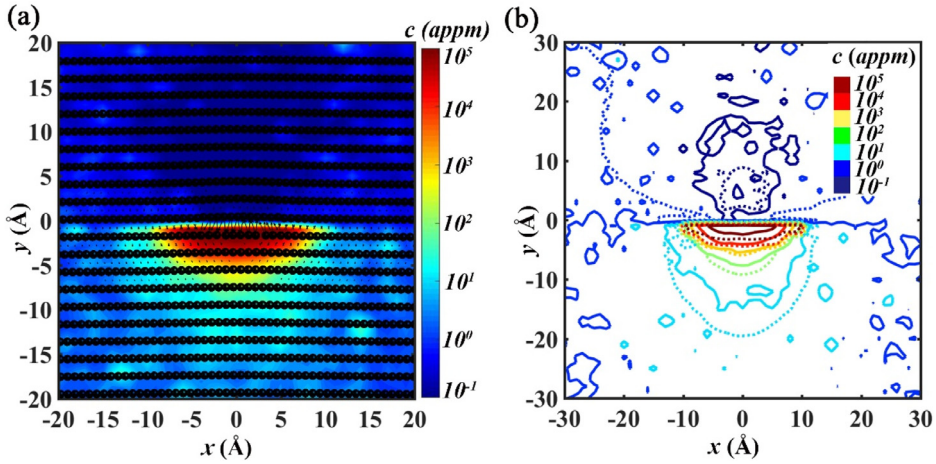

Fig. 1. Core structure of the edge dislocation depicted by differential displacement map in (a) and contour plot of H distribution at $c_0 = 1$ appm in (b). The solid lines are the results of simulations and the dotted lines are the calculations by Eq. (3) using atomistic result of E^{bind}.

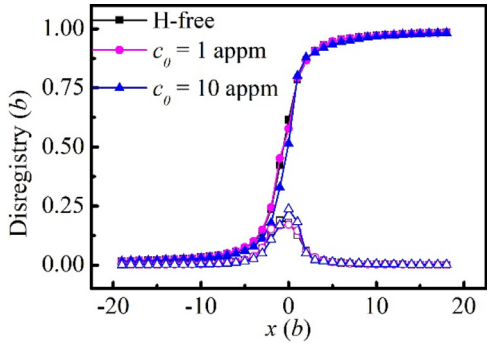

Fig. 2. Disregistry profiles (filled symbols) and distribution of Burgers vector (open symbols) of the edge dislocation with H and without H.

and the same coarse-graining procedure as previous is performed to smooth H concentration around dislocations.

A comparison of H concentration between GCMC simulations and calculations by Eq. (3) for edge dislocation is shown in Fig. 1(b). It is clearly seen that the H concentration obtained by Eq. (3) is higher than that of the GCMC results, indicating that the multiple H–H interaction near the core is repulsive. However, even far away from the core region where H–H interaction is very weak, the simulated H concentration is still lower than that calculated using Eq. (3). This may be attributed to the errors induced by limited MC steps. In the case of screw dislocation, as shown in Fig. 3(b), the simulated H concentration is generally in agreement with the one calculated using Eq. (3), owing to the low H concentration.

As a comparison, we also calculate the H concentration at a site near the edge dislocation according to anisotropic theory. At first, we calculate the binding energy of H with dislocation E^{bind} according to [47]:

$$E^{bind} = v_0 \varepsilon_{ij} \sigma^d, \tag{5}$$

where σ^d is the stress induced by the dislocation and ε_{ij} the strain generated by H within the volume v_0. In the present study, only tetrahedral site is considered to be the trapping site for H. H-induced strain tensors are estimated by $\varepsilon_{11} = \frac{1}{v_0} \frac{C_{11}P_{11} - C_{12}P_{33}}{(C_{11}-C_{12})(C_{11}+2C_{12})}$ and $\varepsilon_{33} = \frac{1}{v_0} \frac{-2C_{12}P_{11} + (C_{12}+C_{11})P_{33}}{(C_{11}-C_{12})(C_{11}+2C_{12})}$ [47]. The obtained results are $\varepsilon_{11} = 0.112$ and $\varepsilon_{33} = 0.056$, and the corresponding volume expansion is 3.57 Å^3, which is in good accordance with the value of 3.818 Å^3 calculated by Song and Curtin [54].

H concentrations around both edge and screw dislocations are then calculated by Eq. (3) using the above obtained results. In the case of the edge dislocation, a comparison of the simulation results with the anisotropic elastic predictions at $c_0 = 1$ appm is shown

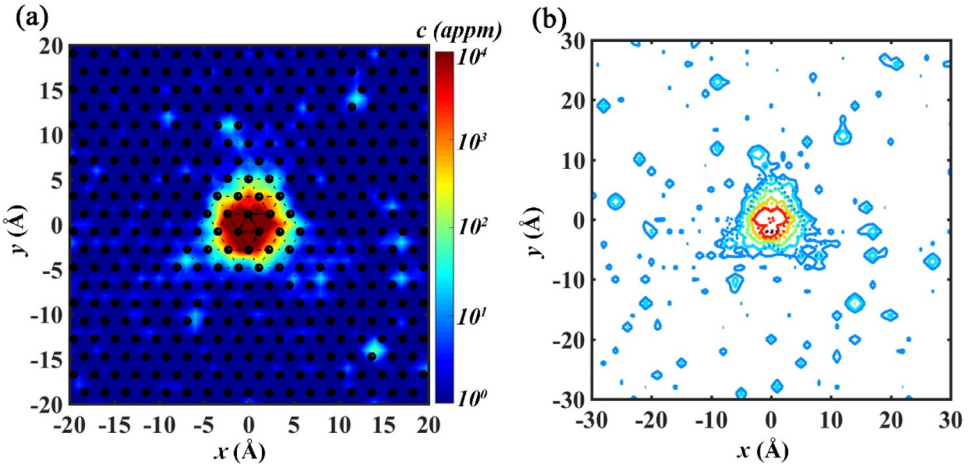

Fig. 3. Core structure of the screw dislocation depicted by differential displacement map in (a) and contour plot of H distribution at $c_0 = 1$ appm in (b). The solid lines are the results of simulations and the dotted lines are the calculations by Eq. (3) using atomistic result of E^{bind}.

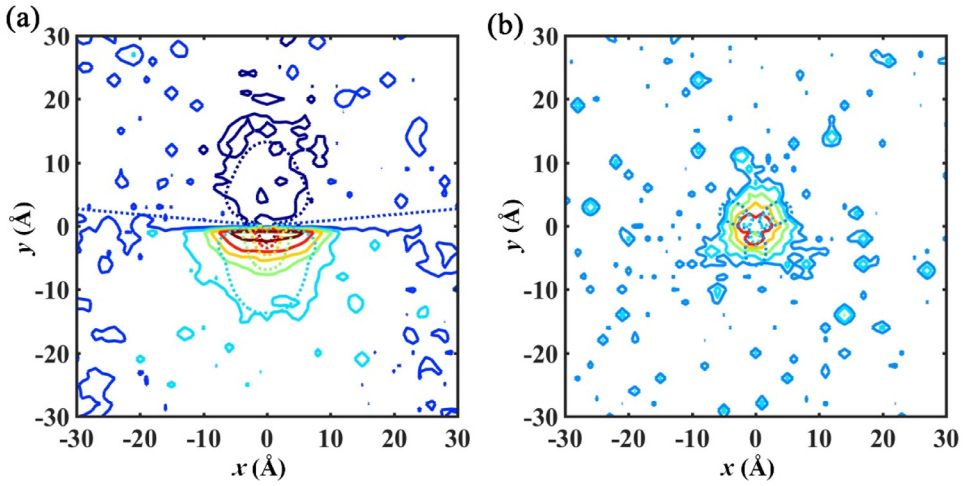

Fig. 4. The contour plot of H distribution for the edge dislocation in (a) and for the screw dislocation in (b) at $c_0 = 1$ appm. The solid lines are the results of simulations and the dotted lines are the calculations by Eq. (3) and (5).

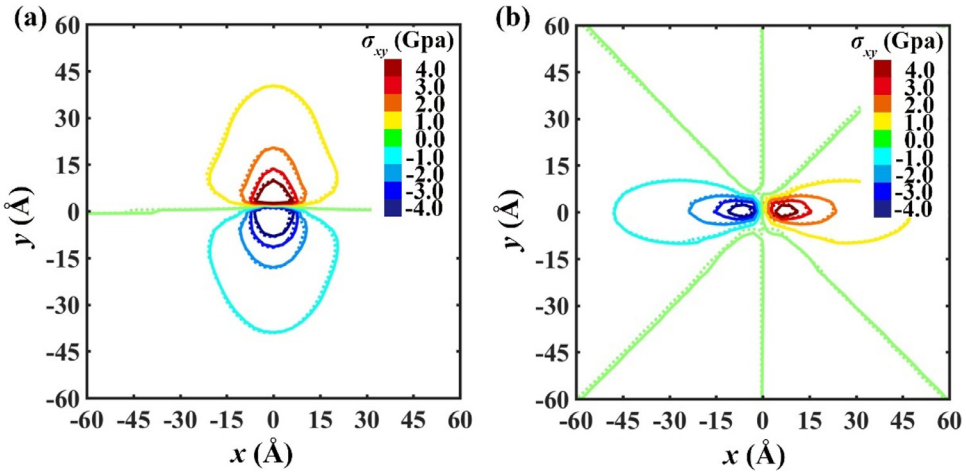

Fig. 5. Contour plot of stress fields of edge dislocation. Solid lines are the contour lines with $c_0 = 1$ appm and dotted lines are those without H. (a) Hydrostatic stress p. (b) Shear stress σ_{xy}.

in Fig. 4(a) by solid lines and dotted lines, respectively. It reveals that the elastically predicted H concentration along the $x = 0$ line and away from the dislocation core region is generally in agreement with the atomistic result. However, due to the extension of the dislocation along the x direction, the atomistic results of H concentrations away from the $x = 0$ line are higher than the elastic predictions. In the case of the screw dislocation, the elastically predicted H distribution pattern, as shown in Fig. 4(b) by dotted lines, is also three-hold symmetrical, in agreement with the atomistic result. However, the elastically predicted H concentration near the dislocation core is underestimated, since the calculated E^{bind} according to Eq. (5) is always lower than the atomistic predicted one.

3.2. H effect on stress distribution

The atomic stress tensor of Fe atoms is calculated by the virial procedure [55]. In a similar way as for the H distribution calculation, the simulation boxes are subdivided into $3 \times 3 \times L$ Å^3 small bins to obtain the stress distributions around dislocations. The obtained contour maps of hydrostatic and shear stresses of both edge and screw dislocations at $c_0 = 1$ appm and those without H as a comparison are shown in Figs. 5 and 6. Clearly, there is nearly no effect of H on the stress fields away from the core regions, as shown in Fig. 5 for the edge dislocation and Fig. 6 for the screw dislocation. This is in line with the study of Cai et al. [56]. Based on the analysis of the isotropic elastic theory, they found that the stress field far from the core of the edge dislocation in Pd is nearly unmodified by H when the bulk H concentration is low.

3.3. H effect on dislocation line energy

The atomistic results of the line energies E of both edge and screw dislocations, in the presence of H, are calculated by

$$E = \frac{1}{L}\left(\sum_i \Delta E_{i,Fe} + \sum_j \Delta E_{j,H}\right), \tag{6}$$

where $\Delta E_{i,\,Fe}$ is the potential energy difference of the ith Fe between the states in the dislocation box and in the perfect bcc lattice, and $\Delta E_{j,\,H}$ the energy difference of the jth H between the states in the dislocation box and in the tetrahedral interstitial site in bcc Fe. The summation runs over all atoms within the radius R from the dislocation center. The final dislocation line energies are the average values over 100 equilibrated snapshots.

It is clear that, as typically shown in Fig. 7, the atomistic line energies of both edge and screw dislocations do vary linearly with logarithmic R in the region with $R > r_c$, as expected from Eq. (1).

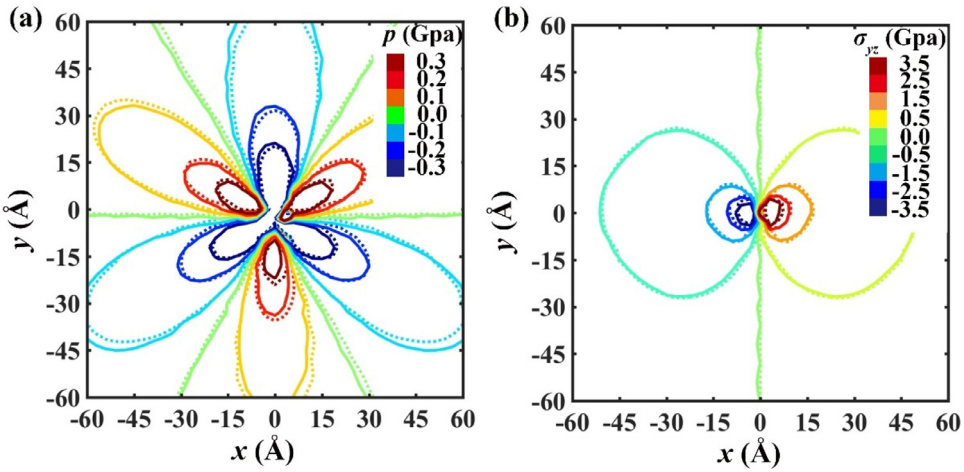

Fig. 6. Contour plot of stress fields of screw dislocation. Solid lines are the contour lines with $c_0 = 1$ appm and dotted lines are those without H. (a) Hydrostatic stress p. (b) Shear stress σ_{yz}.

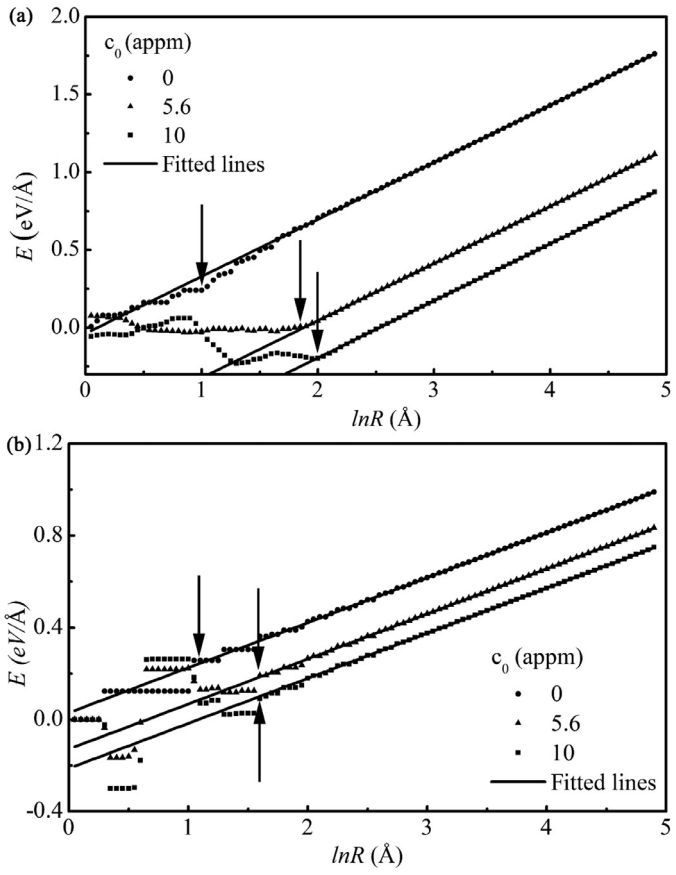

Fig. 7. Dislocation line energies as a function of logarithmic R at $c_0 = 0$, 5.6 and 10 appm for edge dislocation in (a) and screw dislocation in (b). Symbols represent simulation results and lines are the best-fitted ones. Arrows indicate positions that dislocation line energy deviates the fitted lines.

Below r_c, the dislocation line energies E deviate from the linear relationship with lnR because of the large inelastic strain energies of the atoms inside the cores. Thus, we define r_c as the core radius of dislocations.

The energy factor K at each c_0 is obtained by linearly fitting to the E~lnR data in the linear region based on Eq. (1). We find that H has no effect on K, or the crystal elastic constants. The obtained K are 0.75 eVÅ^{-3} for the edge dislocation and 0.40 eVÅ^{-3} for the screw dislocation, which are in perfect agreement with the results calculated by anisotropic elastic theory [41,49]. Considering that the K are obtained from the elastic field of dislocations where the H concentration is extremely low, this result can be reasonably explained. In contrast, Wang et al. [43] found that the shear modulus G for the edge dislocation is reduced by the presence of H. In their simulation, G is obtained by a linear fitting of elastic region in the shear stress versus strain curve in the shear loading process, which is obviously the global value averaged over the whole simulation box (including both the dislocation core and the elastic region) their used. For sure, the G obtained by such a process depends on the size of the simulation box.

Table 1
The obtained dislocation properties. r_c is dislocation core radius, E_c core energies and ΔE the H-induced reduction of dislocation line energy.

Edge						
c_0 (appm)	0	1	1.78	3.16	5.62	10
r_c (Å)	2.9	4.5	5.0	5.6	6.4	7.4
E_c (eV/Å)	0.35	0.28	0.26	0.12	−0.01	−0.19
ΔE (eV/Å)		0.23	0.29	0.49	0.65	0.89
Screw						
r_c (Å)	2.9	2.9	2.9	3.2	5.0	5.0
E_c (eV/Å)	0.24	0.21	0.20	0.19	0.18	0.1
ΔE (eV/Å)		0.03	0.04	0.07	0.16	0.24

The H-induced decreases in the line energies ΔE and the core energies E_c at each c_0 are calculated based on the fitted linear functions. ΔE is defined as the energy difference of the fitted lines between the H-free and the H-charged dislocations at a fixed R in the linear region, and E_c is just the line energy at r_c computed from the fitted linear functions. The results are listed in Table 1. It is evident that for both edge and screw dislocations r_c increases with c_0 while E_c decreases with c_0. The increase of r_c and the decrease of E_c are much more significant for the edge dislocation, owing to the fact that more H atoms are trapped at the edge core because of its stronger H binding energy. The combined effects of H-increased r_c and H-reduced E_c lead to the rapid decrease in the dislocation line energies. This is in agreement with the defactant theory [30–32], according to which H can be thought as a defactant and decrease the formation energy of defects such as grain boundaries, vacancies, dislocations and so on. This is also in agreement with the recent study of Sills et al. on Ni [57] qualitatively. In their work, a constant dislocation core radius is pre-defined and

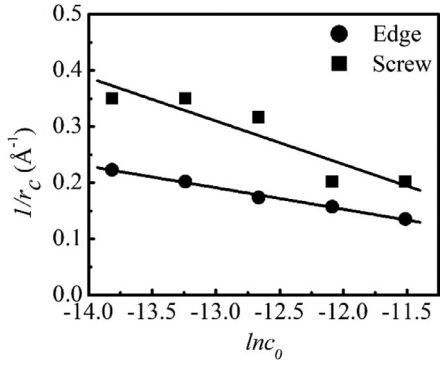

Fig. 8. $1/r_c$ as a function of logarithmic c_0. Symbols represent simulation results and lines represent fitted results.

the free energy change is computed using isotropic elastic theory. The results showed that the core energy is reduced substantially by the formation of hydrides, while the reduction in the energy outside the core is mainly the result of the change of Poisson's ratio. In contrast, in our simulations of H in Fe, the H concentration is much lower than that in Ni, and no hydride formation is observed. Even so, we still observe a significant reduction of dislocation core energy, in line with their result.

4. Discussion

4.1. H effect on dislocation core structure

The dependence of the core radius r_c of the edge dislocation on c_0 can be derived by replacing E^{bind} in Eq. (3) with $p\Delta V$. The pressure p, in the framework of isotropic elastic theory, is given by [41]:

$$p = \frac{\beta sin\,\theta}{r\Delta V}, \tag{7}$$

where r, θ are the cylindrical coordinates with origin at the dislocation center, and β is given by

$$\beta = \frac{Gb(1+\nu)}{3\pi(1-\nu)}\Delta V. \tag{8}$$

In Eq. (8), G is the shear modulus, ν Poisson's ratio, and b the magnitude of Burger vector. In our study, G and ν are obtained by the Voigt average [41] of the single crystal elastic constants given by the EAM potential, which are 89.3 GPa and 0.285 respectively. The volume expansion ΔV of H in the Fe lattice is calculated from the corresponding dipole tensor following the mothed of Schober and Ingle [58], and the obtained value is 3.26 Å^3. Substituting p given in Eq. (7) into Eq. (3) gives:

$$-\frac{kT}{\beta}\left[\ln\frac{c_c}{1-c_c} - \ln c_0\right] = \frac{sin\theta}{r_c}, \tag{9}$$

where c_c is the H concentration at r_c. By setting $\sin\theta = -1.0$, i.e. only considering the situation along the -y direction, a linear dependence of $1/r_c$ on logarithmic c_0 is obtained, if c_c is supposed to be a constant. The variation of $1/r_c$ with logarithmic c_0 and the fitted lines for both edge and screw dislocations are shown in Fig. 8. As shown in the figure, $1/r_c$ is really a linear function of logarithmic c_0 for the edge dislocation. From the linear fitting for the edge dislocation, we obtain a slope of −0.0379 Å^{-1}, which is in close agreement with the predicted value of −0.0302 Å^{-1} by Eq. (9). In the case of the screw dislocation, it is interesting to find that $1/r_c$ is also linearly dependent on logarithmic c_0. However, it changes slowly with logarithmic c_0, mainly due to the low H binding energy to the screw dislocation that the dislocation core is not saturated at low c_0.

4.2. Excess H atmosphere

The excess H is evaluated as the number of H atoms trapped per unit dislocation line length and is averaged from the obtained n_H over 2.4×10^8 microstates generated by GCMC simulations. The atomistic results of the total excess H N within R < 130 Å and the excess H N_e in the elastic field ($r_c < R <$ 130 Å) of the dislocations as a function of logarithmic c_0 are shown in Fig. 9(a) and (b). As is evident, N increases sharply while N_e increases only slowly with logarithmic c_0. The excess H in the elastic field of the dislocations is only a small fraction of the total excess H and can be negligible. Thus, H is mainly trapped at the cores for both edge and screw dislocations, which is qualitatively in agreement with the results of Hirth and Carnahan [59] and Ono and Meshii [60]. Based on their ECNI results and the defactant theory [30–32], Barnoush et al. [18] estimated the excess H N around a dislocation loop in Fe–3 wt% Si as a function of H chemical potential. They obtained an approximately exponential relationship between the excess H and chemical potential, or lnc_0, which is in good agreement with our results in Fig. 9(a) and (b).

As a comparison, we also calculate N_e base on the anisotropic elastic theory, which is given by $N_e = \int_{r_c}^{R} r dr \int_0^{2\pi} (c - c_0) d\theta$ [41]. As shown in Fig. 9(c) and (d), it seems that N_e by atomistic simulations is always higher than that obtained by elastic calculations. Also, we notice that there is a large fluctuation of N_e by atomistic simulations, which is mainly the result of statistic errors.

4.3. H effect on dislocation nucleation

With the development of experimental technology, the interaction of H with dislocations in various metals and alloys has been explored by the in situ ECNI technique. As reviewed by Barnoush et al. [19], the results of ECNI revealed that H enhances HDN in Cu, Al, Ni, Fe–3 wt% Si and FeAl. However, analysis of the ECNI results based on the line tension model still cannot identify whether it is the shear modulus or the core radius of dislocations that is affected by H. Here, the effect of H on HDN in the alloy Fe–3 wt% Si is analyzed and clarified based on the elastic theory and our present atomistic simulations.

In the framework of the elastic theory [41], the free energy ΔG required for the formation of a circular dislocation loop with a loop radius of r is determined by the self-energy of the dislocation loop and the work done by an applied shear stress τ acting on the loop, and is defined as:

$$\Delta G = \frac{Gb^2 r(2-\nu)}{4(1-\nu)}\left(\ln\frac{4r}{r_c} - 2\right) + 2\pi r E_c - \pi r^2 b\tau. \tag{10}$$

The first term in the equation is the elastic energy of the loop, the second one is the core energy and the last one is the work done by τ.

The activation free energy ΔG^*, or the maximum value of ΔG, for the formation of the dislocation loop under a certain τ can be found by setting $\partial\Delta G/\partial r = 0$. As was shown by Barnoush et al. [18–20], since the thermal energy contribution to the HDN is trivial and negligible at room temperature, the applied shear stress τ should be high enough that ΔG^* approaches zero. Thus, the critical shear stress τ_{max} for the formation of a stable loop in HDN can be obtained by solving the simultaneous functions of $\partial\Delta G/\partial r = 0$ and $\Delta G^* = 0$. These give

$$\tau_{\max} = \frac{Gb(2-\nu)}{4\pi(1-\nu)r^*}, \tag{11}$$

with the critical dislocation loop radius

$$r^* = \frac{r_c}{4}\exp\left[3 - \frac{8\pi E_c(1-\nu)}{Gb^2(2-\nu)}\right], \tag{12}$$

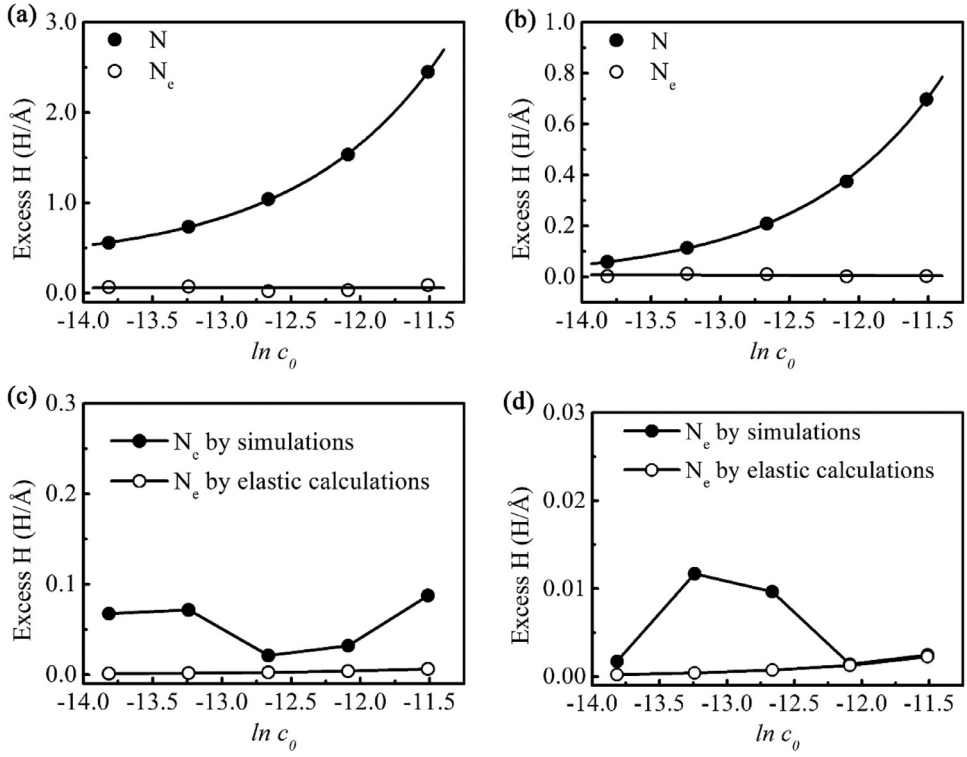

Fig. 9. Excess H as a function of logarithmic c_0 for the edge dislocation in (a) and (c); and for the screw dislocation in (b) and (d).

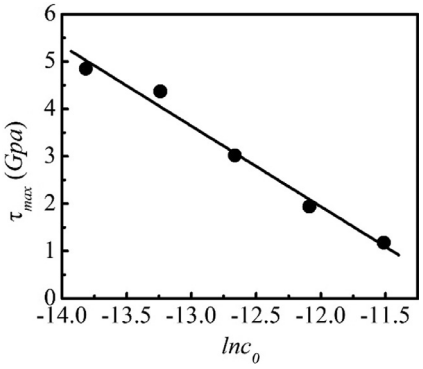

Fig. 10. Critical shear stress of homogeneous dislocation nucleation as a function of logarithmic c_0.

indicating that the H-induced increase in r_c and decrease in E_c lead to the increase in r^* and decrease in τ_{max}.

In order to compare with the ECNI results of Fe–3 wt% Si quantitatively, we adopt the parameters of $G = 85$ GPa and $\nu = 0.3$ from [18]. r_c and E_c are assumed as the averaged values over the edge and screw dislocations by our simulations. The obtained τ_{max} without H is 7.2 GPa, which is 47% higher than the experimental result of 4.9 GPa [19]. This discrepancy may be due to the values of r_c and E_c that are adopted from our simulations of pure Fe. Nevertheless, we obtain $\tau_{max} = 4.85$ GPa at $c_0 = 1$ appm, a decrease by 33% that is in agreement with the experimental result of 27% [18,19], although the exact H concentration by the experiment is unknown. This is also in agreement with the prediction of Sills et al. [57], who found a reduction of τ_{max} by 48% in Ni based on the isotropic elastic analysis.

The calculated τ_{max} as a function of lnc_0 are shown in Fig. 10. It is interesting to note that τ_{max} linearly decreases with increasing lnc_0. The H-induced increase in r_c and decrease in E_c are the reasons for H-enhanced HDN observed by ECNI experiments.

4.4. H effect on interaction between dislocations

Among several mechanisms for HE, the H-enhanced localized plasticity (HELP) is the most discussed and recognized one in recent years. The mechanism is based on the TEM observations that dislocations will move easily in the presence of H, which is attributed to the so-called “shielding” effect that the interaction between dislocations are reduced by the presence of H. However, such a “shielding” effect requires a high bulk H concentration of the order of 10 at%, which is not achievable in non-hydride forming metals and alloys by conventional experimental conditions. Pezold et al. [8] studied the effect of H on the interaction between dislocations in Ni and found that the attractive H–H interaction at a bulk H concentration of 160 appm causes hydride formation in the core of the edge dislocation, which leads to an achievable “shielding” effect suggested by the HELP mechanism only in the case where dislocation spacing is in the order of less than 50 Å. Here, in the case of Fe, the interaction between H atoms is repulsive, thus even at the H concentration of 100 appm that is higher than what can be achieved by conventional experiments of electrolytic charging, we find no effect of H on the stress field of edge and screw dislocations. This is in agreement with the result of Song et al. [54], who studied the effect of H on the dislocation spacing in pile-ups in Fe and found no difference between the H-free and H-charged cases, and it was thus concluded that H will not modify the shear stress distribution in the elastic field of dislocations. This indicates that the effect of H on dislocation interactions can only take place when dislocation cores encounter each other. A direct consequence is that H changes dislocation reactions and the resultant dislocation structures through core-core interaction, which might be the main reason for the mechanism of HELP for HE. According to the present results, this can be easily evaluated by the linear elastic

theory of dislocations, since H only modifies the core radius and energy of dislocations.

5. Conclusions

Atomistic simulations are conducted to investigate the interaction of H with $\frac{1}{2}\langle 111\rangle\{110\}$ edge and screw dislocations in bcc Fe by applying a newly developed EAM potential with the feature of describing the repulsive H–H interaction in the Fe lattice in accord with first principles calculations. GCMC simulations with CB method are conducted to obtain the distribution of H around the dislocations. The effects of H on stress fields, core structures and line energies of dislocations are evaluated and analyzed. Based on these results, the factors leading to the experimentally observed H-enhanced HDN is clarified and the effect of H on the interaction between dislocations is discussed. The conclusions are as follows.

1. There is no change in the shear modulus of the systems containing dislocations, due to the extremely low overall H concentration.
2. Most H atoms are trapped in the cores, resulting in the increase in the core radii and reduction in the core energies of dislocations. The line energies of dislocations are thus decreased.
3. The inverse of the core radius of dislocations decreases linearly with the increase of logarithmic bulk H concentration.
4. H does not modify the stress field of dislocations. Therefore, the interaction between dislocations can only be affected when the separation between dislocations is small enough, i.e., the dislocation cores touch each other.
5. The critical shear stress for HDN decreases linearly with logarithmic bulk H concentration, and the experimentally observed H-enhanced HDN is explained.
6. The H-induced increase in the core radius and decrease in the core energy of dislocations are the key factors affecting dislocation activities including dislocation nucleation, emission, mobility and reaction that leads to HE.
7. The interaction between dislocations in the presence of H can be evaluated by the linear elastic theory using the atomistically determined core radius and energy of dislocations.

Declaration of Competing Interest

None

Acknowledgments

This work was supported by Science Challenge Project (No. TZ2018001) and National Natural Science Foundation of China (Nos. 51271122, 51471107, 51671132).

Supplementary material

Supplementary material associated with this article can be found, in the online version, at doi:10.1016/j.actamat.2019.12.033.

References

[1] W.H. Johnson, On some remarkable changes produced in iron and steel by the action of hydrogen and acids, Proc. R. Soc. Lond. 23 (1875) 156–163.
[2] R.D. Merrick, Overview of hydrogen damage to steels at low temperatures, Mater. Perform. 28 (1989) 53–55.
[3] I.M. Robertson, The effect of hydrogen on dislocation dynamics, Eng. Fract. Mech. 68 (2001) 671–692.
[4] S.M. Myers, M.I. Baskes, H.K. Birnbaum, J.W. Corbett, G.G. Deleo, S.K. Estreicher, E.E. Haller, P. Jena, N.M. Johnson, R. Kirchheim, S.J. Pearton, M.J. Stavola, Hydrogen interactions with defects in crystalline solids, Rev. Mod. Phys. 64 (1992) 559–617.
[5] J. Lufrano, P. Sofronis, H.K. Birnbaum, Modeling of hydrogen transport and elastically accommodated hydride formation near a crack tip, J. Mech. Phys. Solids 44 (1996) 179–205.
[6] R.A. Oriani, P.H. Josephic, Equilibrium and kinetic studies of the hydrogen-assisted cracking of steel, Acta Metall. 25 (1977) 979–988.
[7] H.K. Birnbaum, P. Sofronis, Hydrogen-enhanced localized plasticity-a mechanism for hydrogen-related fracture, Mater. Sci. Eng. A 176 (1994) 191–202.
[8] J.V. Pezold, L. Lymperakis, J. Neugebeauer, Hydrogen-enhanced local plasticity at dilute bulk H concentrations: the role of H–H interactions and the formation of local hydrides, Acta Mater. 59 (2011) 2969–2980.
[9] M. Nagumo, Hydrogen related failure of steels-a new aspect, Meter. Sci. Technol. 20 (2004) 940–950.
[10] I.M. Robertson, H.K. Birnbaum, An HVEM study of hydrogen effects on the deformation and fracture of nickel, Acta Metall. 34 (1986) 353–366.
[11] K.A. Nibur, D.F. Bahr, B.P. Somerday, Hydrogen effects on dislocation activity in austenitic stainless steel, Acta Mater. 54 (2006) 2677–2684.
[12] Y. Takahashi, M. Tanaka, K. Higashida, K. Yamaguchi, H. Noguchi, An intrinsic effect of hydrogen on cyclic slip deformation around a {1 1 0} fatigue crack in Fe–3.2wt% Si alloy, Acta Mater. 58 (2010) 1972–1981.
[13] P.J. Ferreira, I.M. Robertson, H.K. Birnbaum, Hydrogen effects on the interaction between dislocations, Acta Mater. 46 (1998) 1749–1757.
[14] D.S. Shih, I.M. Robertson, H.K. Birnbaum, Hydrogen embrittlement of alpha titanium: in situ TEM studies, Acta Metall. 36 (1988) 111–124.
[15] M.L. Martin, J.A. Fenske, G.S. Liu, P. Sofronis, I.M. Robertson, On the formation and nature of quasi-cleavage fracture surfaces in hydrogen embrittled steels, Acta Mater. 59 (2011) 1601–1606.
[16] T. Neeraj, R. Srinivasan, J. Li, Hydrogen embrittlement of ferritic steels: observations on deformation microstructure, nanoscale dimples and failure by nanovoiding, Acta Mater. 60 (2012) 5160–5171.
[17] M.L. Martin, B.P. Somerday, R.O. Ritchie, P. Sofronis, I.M. Robertson, Hydrogen-induced intergranular failure in nickel revisited, Acta Mater. 60 (2012) 2739–2745.
[18] A. Barnoush, N. Kheradmand, T. Hajilou, Correlation between the hydrogen chemical potential and pop-in load during in situ electrochemical nanoindentation, Scr. Mater. 108 (2015) 76–79.
[19] A. Barnoush, H. Vehoff, Recent developments in the study of hydrogen embrittlement: hydrogen effect on dislocation nucleation, Acta Mater. 58 (2010) 5274–5285.
[20] A. Barnoush, M. Asgari, R. Johnsen, Resolving the hydrogen effect on dislocation nucleation and mobility by electrochemical nanoindentation, Scr. Mater. 66 (2012) 414–417.
[21] A.H. Cottrell, M.A. Jaswon, Distribution of solute atoms round a slow dislocation, Proc. R. Soc. Lond. A 199 (1949) 104–114.
[22] A.H. Cottrell, Dislocations and plastic flow in crystals, Am. J. Phys. 22 (1954) 242.
[23] J.D. Eshelby, The determination of the elastic field of an ellipsoidal inclusion, and related problems, Proc. R. Soc. Lond. A 241 (1957) 376–396.
[24] F.C. Larché, J.W. Cahn, The interactions of composition and stress in crystalline solids, Acta Metall. 33 (1985) 331–357.
[25] Y. Mishin, J.W. Cahn, Thermodynamics of Cottrell atmospheres tested by atomistic simulations, Acta Mater. 117 (2016) 197–206.
[26] S. Taketomi, R. Matsumoto, N. Miyazaki, Atomistic simulation of the effects of hydrogen on the mobility of edge dislocation in alpha iron, J. Mater. Sci. 43 (2008) 1166–1669.
[27] S. Taketomi, R. Matsumoto, N. Miyazaki, Atomistic study of hydrogen distribution and diffusion around a {112}<111>edge dislocation in alpha iron, Acta Mater. 56 (2008) 3761–3769.
[28] M. Wen, S. Fukuyama, K. Yokogawa, Atomistic simulations of effect of hydrogen on kink-pair energetics of screw dislocations in bcc iron, Acta Mater. 51 (2003) 1767–1773.
[29] T. Lu, Y.-P. Xu, X.-D. Pan, H.-S. Zhou, F. Ding, Z.S. Yang, G.-J. Niu, G.-N. Luo, X.-C. Li, F. Gao, Atomistic study of hydrogen behavior around dislocations in α iron, J. Nucl. Mater. 510 (2018) 219–228.
[30] R. Kirchheim, Reducing grain boundary, dislocation line and vacancy formation energies by solute segregation. I. Theoretical background, Acta Mater. 55 (2007) 5129–5138.
[31] R. Kirchheim, Reducing grain boundary, dislocation line and vacancy formation energies by solute segregation. II. Experimental evidence and consequences, Acta Mater. 55 (2007) 5139–5148.
[32] R. Kirchheim, On the solute-defect interaction in the framework of a defactant concept, Int. J. Mater. Res. 100 (2009) 483–487.
[33] R. Kirchheim, Solid solution softening and hardening by mobile solute atoms with special focus on hydrogen, Scr. Mater. 67 (2012) 767–770.
[34] M. Deutges, H.P. Barth, Y.Z. Chen, C. Borchers, R. Kirchheim, Hydrogen diffusivities as a measure of relative dislocation densities in palladium and increase of the density by plastic deformation in the presence of dissolved hydrogen, Acta Mater. 82 (2015) 266–274.
[35] C.M. Sturges, A.P. Miodownik, The interaction of hydrogen and dislocations in iron, Acta Metall. 17 (1969) 1197–1207.
[36] W.M. Robertson, Measurement and evaluation of hydrogen trapping in thoria dispersed nickel, Metall. Trans. A 10 (1979) 489–501.
[37] B.J. Heuser, D.R. Trinkle, T.-N. Yang, L.L. He, Hydrogen trapping at dislocation cores at room temperature in deformed PD, J. Alloys Compd. 577 (2013) 189–191.
[38] Y. Zhao, G. Lu, QM/MM study of dislocation-hydrogen/helium interactions in α-Fe, Model. Simul. Mater. Sci. Eng. 19 (2011) 065004.
[39] Y.Z. Tang, J.A. El-Awady, Atomistic simulations of the interactions of hydrogen with dislocations in fcc metals, Phys. Rev. B 86 (2012) 174102.

[40] M. Itakura, H. Kaburaki, M. Yamaguchi, T. Okita, The effect of hydrogen atoms on the screw dislocation mobility in bcc iron: a first-principles study, Acta Mater. 61 (2013) 6857–6867.
[41] J.P. Hirth, J. Lothe, Theory of Dislocations, 2nd ed., Wiley, New York, 1982.
[42] G. Lu, Q. Zhang, N. Kioussis, E. Kaxiras, Hydrogen-enhanced local plasticity in aluminum: an ab initio study, Phys. Rev. Lett. 87 (2001) 095501.
[43] S. Wang, N. Hashimoto, S. Ohnuki, Hydrogen-induced change in core structures of {110}[111]edge and {110}[111]screw dislocations in iron, Sci. Rep. 3 (2013) 2760.
[44] G.J. Ackland, M.I. Mendelev, D.J. Srolovitz, S. Han, A.V. Barashev, Development of an interatomic potential for phosphorus impurities in α-iron, J. Phys.: Condens. Matter 16 (2004) S2629–S2642.
[45] A. Ramasubramaniam, M. Itakura, E.A. Carter, Interatomic potentials for hydrogen in α-iron based on density functional theory, Phys. Rev. B 79 (2009) 174101.
[46] J. Song, W.A. Curtin, Atomic mechanism and prediction of hydrogen embrittlement in iron, Nat. Mater. 12 (2013) 145–151.
[47] E. Clouet, S. Garruchet, H. Nguyen, M. Perez, C.S. Becquart, Dislocation interaction with C in a-Fe: a comparison between atomic simulations and elasticity theory, Acta Mater. 56 (2008) 3450–3460.
[48] X. Li, C. Gao, X.L. Xiong, Y. Bai, Y.J. Su, Hydrogen diffusion in a-Fe under an applied 3-axis strain: a quantum manifestation, Int. J. Hydrogen Energy 40 (2015) 10340–10345.
[49] D.J. Bacon, D.M. Barnett, R.O. Scattergood, Anisotropic continuum theory of lattice defects, Prog. Mater. Sci. 23 (1980) 51–262.
[50] D.J. Adams, Grand canonical ensemble Monte Carlo for a Lennard–Jones fluid, Mol. Phys. 29 (1975) 307–311.
[51] M. Mezei, A cavity-biased (T, V, μ) Monte Carlo method for the computer simulation of fluids, Mol. Phys. 40 (1980) 901–906.
[52] M. Wen, L. Zhang, B. An, S. Fukuyama, K. Yokogawa, Hydrogen-enhanced dislocation activity and vacancy formation during nanoindentation of nickel, Phys. Rev. B 80 (2009) 094113.
[53] C. Goldenberg, A. Tanguy, J.-L. Barrat, Particle displacements in the elastic deformation of amorphous materials: local fluctuations vs. non-affine field, EPL 80 (2007) 16003.
[54] J. Song, W.A. Curtin, Mechanisms of hydrogen-enhanced localized plasticity: an atomistic study using α-Fe as a model system, Acta Mater. 68 (2014) 61–69.
[55] D.H. Tsai, The virial theorem and stress calculation in molecular dynamics, J. Chem. Phys. 70 (1979) 1375.
[56] W. Cai, R.B. Sills, D.M. Barnett, W.D. Nix, Modeling a distribution of point defects as misfitting inclusions in stressed solids, J. Mech. Phys. Solids 66 (2014) 154–171.
[57] R.B. Sills, W. Cai, Free energy change of a dislocation due to a Cottrell atmosphere, Philos. Mag. 98 (2018) 1491–1510.
[58] H.R. Schober, K.W. Ingle, Calculation of relaxation volumes, dipole tensors and Kanzaki forces for point defects, J. Phys. F: Metal Phys. 10 (1980) 575–581.
[59] J.P. Hirth, B. Carnahan, Hydrogen adsorption at dislocations and cracks in Fe, Acta Metall. 26 (1978) 1795–1803.
[60] K. Ono, M. Meshii, Hydrogen detrapping from grain boundaries and dislocations in high purity iron, Acta Metall. Mater. 40 (1992) 1357–1364.